Proceeding Series of the Brazilian Society of Computational and Applied Mathematics, v. 10, n. 1, 2023.

Trabalho apresentado no XLII CNMAC, Universidade Federal de Mato Grosso do Sul - Bonito - MS, 2023

Proceeding Series of the Brazilian Society of Computational and Applied Mathematics

Investigation of non-smooth solutions in finite elasticity using the phase-plane method

Adair R. Aguiar[1], Lucas A. Rocha[2]
EESC/USP, São Carlos, SP

Abstract. We use the phase-plane method to investigate a class of problems in finite elasticity for which the spatial derivative of a solution may have a finite jump at an interior point of the domain. In particular, we consider the equilibrium of a nonlinearly elastic annular disk fixed on its inner surface and subjected to a constant uniform pressure on its outer surface. We show that the solution of this problem is non-differentiable at an interior point when the applied pressure exceeds a certain value. This value serves as an upper bound for the pressure that can be applied without violating the range of validity of the infinitesimal theory. On the other hand, non-smooth deformation fields are of interest in the study of crystalline materials that can exist in more than one crystal structure, such as the shape-memory alloys.

Keywords. Phase-Plane Method, Phase Portrait, Finite Elasticity, Anisotropy

1 Introduction

Problems of interest in mechanics are described by nonlinear differential equations, for which determining a solution in closed form or verifying the existence and uniqueness of solutions is not a simple task. In such cases, it is common to use numerical methods to obtain approximate solutions. However, numerical methods may not provide all the possible solutions. The undetected solutions may occur in real applications and cause an unexpected failure of a component, such as buckling of a bar. To avoid that, we can use tools of the qualitative theory of differential equations to better understand the problem at hand. For instance, the phase-plane method yields a graphical tool to study the properties of solutions of differential equations.

In this work, we use the phase-plane method to investigate a class of problems in finite elasticity for which the spatial derivative of a solution may have a finite jump at an interior point of the domain depending on the applied boundary condition. This investigation yields qualitative results that are very helpful in the selection of adequate numerical strategies for the approximate solution of differential equations.

In particular, we consider the problem of an elastic annular disk with uniform thickness in equilibrium in the absence of body force. The disk is fixed on its inner surface of radius $R_i > 0$ and compressed by a constant and uniform pressure $p > 0$ on its outer surface of radius $R_e > R_i$. The disk is made of a transversely isotropic material with a radial symmetry axis.

In the context of the classical linear theory of elasticity, the solution of the disk problem is unique and, for $R_i = 0$, predicts that the stresses go monotonically to minus infinity as we approach the center of the disk, even for small values of p, [4]. In this theory, large stresses imply large strains, which violates the hypothesis of infinitesimal strains on which the theory is based upon.

In the context of the finite elasticity theory, Antman and Negrón-Marrero [2] have studied the disk problem in the case $R_i = 0$ and have used the phase-plane method to show that the stresses

[1] aguiarar@sc.usp.br
[2] lucas.almeida.rocha@usp.br

also go monotonically to minus infinity at the center of the disk. The authors have not completely characterized the elastic material. Instead, they have made some physical assumptions about its elastic response. Although these assumptions are general and suitable for many materials, it includes certain conditions that preclude non-monotonic relations between stresses and stretches. This type of non-monotonic response is of interest in the investigation of solids that undergo a deformed state with multiple solid phases, such as the shape-memory alloy NiTi and the ferroelectric alloy $BaTiO_3$, [1]. We consider that the disk is made of an anisotropic St Venant-Kirchhoff material, which corresponds to a natural constitutive extension of the infinitesimal to the finite elasticity theory. In addition, this material model has a non-monotonic relation between radial stress and radial stretch.

In Section 2 we present some background material about the finite elasticity theory and formulate the disk problem. In Section 3 we use the phase-plane method to study the solution of the disk problem. In Section 4 we present some concluding remarks.

2 The Disk Problem

Let $\mathcal{B} \subset \mathbb{R}^3$ denote the undistorted reference configuration of a nonlinearly elastic solid in equilibrium. Points $\mathbf{x} \in \mathcal{B}$ are mapped into points $\mathbf{y} \triangleq \mathbf{f}(\mathbf{x})$, where $\mathbf{f} : \mathcal{B} \to \mathbb{R}^3$ is the deformation field. The boundary $\partial\mathcal{B}$ of $\mathcal{B}$ is composed of two non-intersecting parts, $\partial_1\mathcal{B}$ and $\partial_2\mathcal{B}$, $\partial\mathcal{B} = \partial_1\mathcal{B} \cup \partial_2\mathcal{B}$, $\partial_1\mathcal{B} \cap \partial_2\mathcal{B} = \emptyset$, such that $\mathbf{f}(\mathbf{x}) = \bar{\mathbf{f}}(\mathbf{x})$ for $\mathbf{x} \in \partial_1\mathcal{B}$, where $\bar{\mathbf{f}}$ is a given function, and the traction field $\bar{\mathbf{t}}(\mathbf{x})$ is prescribed for $\mathbf{x} \in \partial_2\mathcal{B}$.

The first Piola-Kirchhoff stress tensor at $\mathbf{x}$, denoted by $\mathbf{P}(\mathbf{x}) \in \mathrm{Lin}$, is related to the deformation $\mathbf{f}$ by $\mathbf{P}(\mathbf{x}) = \hat{\mathbf{P}}(\mathbf{x}, \nabla\mathbf{f}(\mathbf{x}))$, where $\hat{\mathbf{P}} : \mathcal{B} \times \mathrm{Lin} \to \mathrm{Lin}$ is the response function of the material, ∇ is the gradient operator with respect to $\mathbf{x}$, and Lin is the space of linear transformations defined on $\mathbb{R}^3$.

In the absence of body force, the deformation field $\mathbf{f}$ must satisfy the equilibrium equation

$$\mathrm{Div}\,\hat{\mathbf{P}}(\mathbf{x}, \nabla\mathbf{f}(\mathbf{x})) = \mathbf{0}\,, \qquad \mathbf{x} \in \mathcal{B}\,, \tag{1}$$

and the boundary conditions

$$\mathbf{f}(\mathbf{x}) = \bar{\mathbf{f}}(\mathbf{x})\,, \text{ for } \mathbf{x} \in \partial_1\mathcal{B}\,, \qquad \hat{\mathbf{P}}(\mathbf{x}, \nabla\mathbf{f}(\mathbf{x}))\,\mathbf{N} = \bar{\mathbf{t}}(\mathbf{x})\,, \text{ for } \mathbf{x} \in \partial_2\mathcal{B}\,, \tag{2}$$

where Div is the divergence operator with respect to $\mathbf{x}$ and $\mathbf{N} \in \mathbb{R}^3$ is the outer unit normal vector to $\partial_2\mathcal{B}$ at $\mathbf{x}$.

We assume that the material is hyperelastic, so that

$$\hat{\mathbf{P}} = \partial W/\partial\mathbf{F}\,, \tag{3}$$

where $W = W(\mathbf{x}, \mathbf{F})$ is the strain energy density function of the material, $\mathbf{F} \triangleq \nabla\mathbf{f}$, and $\partial(\cdot)/\partial\mathbf{F}$ is the gradient operator with respect to $\mathbf{F}$. Near the reference configuration, where deformations are small but not necessarily infinitesimal, W can be written as

$$W = \frac{1}{2}\,\mathbf{E} \cdot \mathbb{C}[\mathbf{E}]\,, \qquad \mathbf{E} \triangleq \frac{1}{2}\,(\mathbf{F}^T\,\mathbf{F} - \mathbf{I})\,, \tag{4}$$

where $\mathbf{E}$ is the Green St Venant strain tensor and $\mathbb{C}$ is the elasticity tensor. If the material is isotropic, then it is the classical St Venant-Kirchhoff material; otherwise, we call it the *anisotropic St Venant-Kirchhoff material*.

Let $\{\mathbf{e}_R, \mathbf{e}_\Theta, \mathbf{e}_Z\}$ denote the usual orthonormal cylindrical basis at $\mathbf{x}$ associated with the cylindrical coordinates (R, Θ, Z), such that $\mathbf{x} = R\,\mathbf{e}_R(\Theta) + Z\,\mathbf{e}_Z$. Similarly, let $\{\mathbf{e}_r, \mathbf{e}_\theta, \mathbf{e}_z\}$ and (r, θ, z)

be the corresponding orthonormal cylindrical basis and coordinates, respectively, at $\mathbf{y}$, such that $\mathbf{y} = r\,\mathbf{e}_r(\theta) + z\,\mathbf{e}_z$. We shall omit the dependence of $\mathbf{e}_R$ and $\mathbf{e}_r$ on Θ and θ, respectively.

We consider the equilibrium problem of a nonlinearly elastic annular disk with uniform thickness h. The disk is fixed on its inner surface of radius $R_i > 0$ and compressed by a constant and uniform pressure $p > 0$ on its outer surface of radius $R_e > R_i$. The disk is made of an anisotropic St Venant-Kirchhoff material that is transversely isotropic with respect to the radial direction. Therefore, its strain energy density function is given by (4), where the nonzero components of the elasticity tensor $\mathbb{C}$ with respect to $\{\mathbf{e}_R, \mathbf{e}_\Theta, \mathbf{e}_Z\}$ are constant and given by the elastic moduli $c_{11}, c_{12}, c_{22}, c_{23}, c_{66}$. All lengths can be rendered dimensionless by normalizing them with respect to R_e, so that $\mathbf{x} = (R, \Theta, Z) \in [\alpha, 1] \times [0, 2\pi] \times [0, \beta]$, where $\alpha \triangleq R_i/R_e$ and $\beta \triangleq h/R_e$.

We want to find a radially symmetric deformation field $\mathbf{f}$, such that points $\mathbf{x} \in \mathcal{B}$ move along radial lines according to

$$\mathbf{f}(R, \Theta, Z) = r(R)\,\mathbf{e}_r + Z\,\mathbf{e}_z\,. \tag{5}$$

Since $\mathbf{F} \triangleq \nabla\mathbf{f}$, we have that

$$\mathbf{F} = \nu(R)\,\mathbf{e}_r \otimes \mathbf{e}_R + \tau(R)\,\mathbf{e}_\theta \otimes \mathbf{e}_\Theta + \mathbf{e}_z \otimes \mathbf{e}_Z\,, \qquad \nu(R) \triangleq r'(R)\,, \quad \tau(R) \triangleq r(R)/R\,, \tag{6}$$

where the explicit dependence on $\mathbf{x} = (R, \Theta, Z)$ is omitted and $(\cdot)'$ denotes the derivative with respect to R. In view of (5), the dimensionless thickness β has no influence on the results of this work. Substituting (6) into (4) and then using the resulting expression together with (3), we arrive at

$$\mathbf{P} = P_{rr}(R)\,\mathbf{e}_r \otimes \mathbf{e}_R + P_{\theta\theta}(R)\,\mathbf{e}_\theta \otimes \mathbf{e}_\Theta + P_{zz}(R)\,\mathbf{e}_z \otimes \mathbf{e}_Z\,, \tag{7}$$

$$P_{rr}(R) = \hat{P}_{rr}(\tau, \nu) = \left[c_{11}\,(\nu^2 - 1) + c_{12}\,(\tau^2 - 1)\right]\nu/2, \tag{8}$$

$$P_{\theta\theta}(R) = \hat{P}_{\theta\theta}(\tau, \nu) = \left[c_{12}\,(\nu^2 - 1) + c_{22}\,(\tau^2 - 1)\right]\tau/2\,, \tag{9}$$

$$P_{zz}(R) = \hat{P}_{zz}(\tau, \nu) = \left[c_{12}\,(\nu^2 - 1) + c_{23}\,(\tau^2 - 1)\right]/2\,. \tag{10}$$

Substituting (7) into the vector equilibrium equation (1), we find that this equation reduces to the scalar ordinary differential equation given by

$$\frac{d}{dR}\left[R\,P_{rr}(R)\right] - P_{\theta\theta}(R) = 0\,. \tag{11}$$

Also, the boundary conditions in (2) for the disk problem take the form

$$r(\alpha) = \alpha\,, \qquad P_{rr}(1) = -p\,r(1)\,, \tag{12}$$

where the pressure $p > 0$ is constant and uniform in the deformed configuration.

Thus, the *disk problem* of this work consists of finding $r : [\alpha, 1] \to \mathbb{R}$ that satisfies the ordinary differential equation (11) together with (6), (8), (9), and the boundary conditions (12).

3 Phase Portraits

Phase portraits are diagrams used in the study of properties of solutions of differential equations. We begin by constructing the phase portrait of the differential equation (11) for an arbitrary material and then particularize it for the anisotropic St Venant-Kirchhoff material by using the stress relations (8) and (9).

Let us assume that $\hat{P}_{rr}(\tau, \cdot)$ has an inverse given by $\check{\nu}(\tau, \cdot)$, such that if $P_{rr} = \hat{P}_{rr}(\tau, \nu)$, then $\nu = \check{\nu}(\tau, P_{rr})$. We then define $\check{P}_{\theta\theta}(\tau, P_{rr}) \triangleq \hat{P}_{\theta\theta}(\tau, \check{\nu}(\tau, P_{rr}))$ and rewrite the differential equation (11) as the system of equations

$$\frac{d}{dR}[R\,\tau] = \check{\nu}(\tau, P_{rr})\,, \qquad \frac{d}{dR}[R\,P_{rr}(R)] = \check{P}_{\theta\theta}(\tau, P_{rr})\,. \tag{13}$$

Next, we do the change of variable $R = e^{\xi}$, so that $\xi \in [\log \alpha, 0]$, and rewrite $\tau(e^{\xi})$ as $\tau(\xi)$ and $P_{rr}(e^{\xi})$ as $P_{rr}(\xi)$. The system of equations (13) can then be rewritten as the system of autonomous equations given by

$$d\tau/d\xi = \check{\nu}(\tau, P_{rr}) - \tau\,, \qquad dP_{rr}/d\xi = \check{P}_{\theta\theta}(\tau, P_{rr}) - P_{rr}\,, \tag{14}$$

where we have omitted the dependence of both τ and P_{rr} on ξ.

To construct the phase portrait of the autonomous system (14) in the plane $\mathcal{U} \triangleq \{(\tau, P_{rr}) \mid \tau,\, P_{rr} \in \mathbb{R}\}$, we must determine expressions for $\check{\nu}(\tau, P_{rr})$ and $\check{P}_{\theta\theta}(\tau, P_{rr})$. From (8), we see that $\nu = \check{\nu}(\tau, P_{rr})$ satisfies the cubic equation

$$\nu^3 - \left[1 + (1-\tau^2)\, c_{12}/c_{11}\right] \nu - 2\, P_{rr}/c_{11} = 0. \tag{15}$$

The discriminant of this equation is given by

$$D = D(\tau, P_{rr}) \triangleq -4\, a^3 - 27\, b^2\,, \tag{16}$$

where $a \triangleq -[1+(1-\tau^2)\, c_{12}/c_{11}]$ and $b \triangleq -2\, P_{rr}\, /c_{11}$. If $D > 0$, the equation (15) has three distinct real roots; if $\mathcal{D} < 0$, it has only one real root; if $D = 0$, it may have one or two distinct real roots. We use D to define the regions $\mathcal{D}_{>} \triangleq \{(\tau, P_{rr}) \in \mathcal{U} \mid D > 0\}$ and $\mathcal{D}_{<} \triangleq \{(\tau, P_{rr}) \in \mathcal{U} \mid D < 0\}$. The interface between $\mathcal{D}_{>}$ and $\mathcal{D}_{<}$ corresponds to the points where $D = 0$. Once $\nu = \check{\nu}(\tau, P_{rr})$ is determined, $\check{P}_{\theta\theta}(\tau, P_{rr})$ is obtained from (9) by recalling its definition from above.

Next, we use the boundary conditions (12) to define the *initial curve* $\mathcal{C}_i$ and the *terminal curve* $\mathcal{C}_e$ as, respectively,

$$\mathcal{C}_i \triangleq \{(\tau, P_{rr}) \in \mathcal{U} \mid \tau = 1\}, \qquad \mathcal{C}_e \triangleq \{(\tau, P_{rr}) \in \mathcal{U} \mid P_{rr} = -p\,\tau\}\,. \tag{17}$$

A *trajectory* of the system (14) is a curve in $\mathcal{U}$ parameterized by ξ that satisfies (14) and is oriented according to increasing values of ξ. The *trajectory of the solution* of the disk problem is a segment of a trajectory of the system (14) that begins at the initial curve $\mathcal{C}_i$, which corresponds to $\xi = \log \alpha$, and ends at the terminal curve $\mathcal{C}_e$, which corresponds to $\xi = 0$.

Singular points of the system (14) are points where both the vertical isocline $\mathcal{V} \triangleq \{(\tau, P_{rr}) \in \mathcal{U} \mid d\tau/d\xi = 0 \overset{(14)}{\iff} \check{\nu}(\tau, P_{rr}) = \tau\}$ and the horizontal isocline $\mathcal{H} \triangleq \{(\tau, P_{rr}) \in \mathcal{U} \mid dP_{rr}/d\xi = 0 \overset{(14)}{\iff} \check{P}_{\theta\theta}(\tau, P_{rr}) = P_{rr}\}$ intersect. It is not difficult to show that these points are such that $\hat{P}_{\theta\theta}(\tau, \tau) = \hat{P}_{rr}(\tau, \tau)$. Therefore, from (8)-(9), we expect singular points at $(\tau, P_{rr}) \in \{(-1, 0), (0, 0), (1, 0)\}$.

In the remainder of this work, we use the following engineering constants: $E_1 = 15$, $E_2 = 1$, $\mathrm{v}_{12} = 0.25, \mathrm{v}_{23} = 0.5$, where E and v denote the Young's modulus and the Poisson ratio, respectively, and the subscripts 1, 2, and 3 denote the radial, tangential, and axial directions, respectively. These values of E_1 and E_2 multiplied by a factor of 10^{10} in pascal (Pa) can be used to approximately represent the constants of a unidirectional carbon/epoxy composite, [3]. Using the relations $c_{11} = E_1\,(1 - \mathrm{v}_{23})/m$, $c_{12} = E_2\,\mathrm{v}_{12}/m$, and $c_{22} = E_2\,\left(1 - \mathrm{v}_{12}^2\, E_2/E_1\right)/\left[m\,(1 + \mathrm{v}_{23})\right]$, where $m \triangleq 1 - \mathrm{v}_{23} - 2\,\mathrm{v}_{12}^2\, E_2/E_1$, we obtain $c_{11} \approx 15.2542$, $c_{12} \approx 0.508475$, and $c_{22} \approx 1.35028$.

In Figure 1 we plot the phase portrait associated with the system (14), which consists of a collection of trajectories of the system together with some auxiliary lines defined below. As mentioned in the previous section, at $(\tau, P_{rr}) \in \mathcal{D}_{>}$, which is the region delimited by the green dashed lines, $\nu = \check{\nu}(\tau, P_{rr})$ may assume three possible values. Figures 1a, 1b, and 1c are phase portraits obtained by choosing ν as the minimum, intermediate, and maximum real root of (15), respectively, which imply that trajectories differ only inside $\mathcal{D}_{>}$. The gray oriented lines are the trajectories, the black vertical line is $\mathcal{C}_i$, given by (17.a), the blue slightly inclined line is $\mathcal{C}_e$, given by (17.b), for $p = 0.05$, and the black dotted line corresponds to $P_{rr} = 0$.

DOI: 10.5540/03.2023.010.01.0064

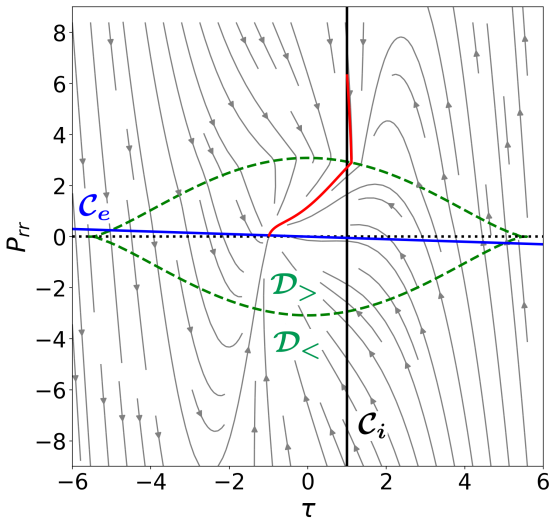

(a) Minimum real root

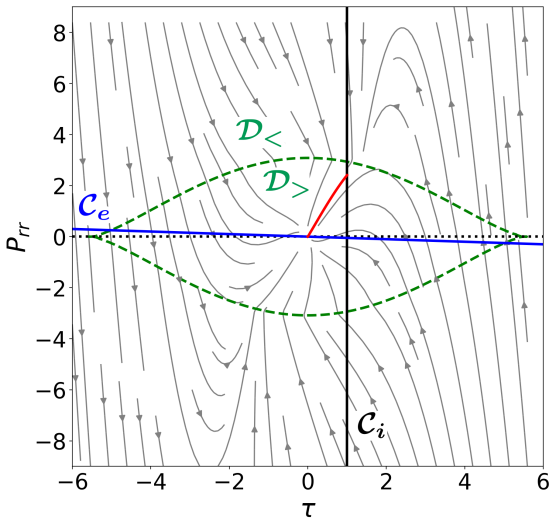

(b) Intermediate real root

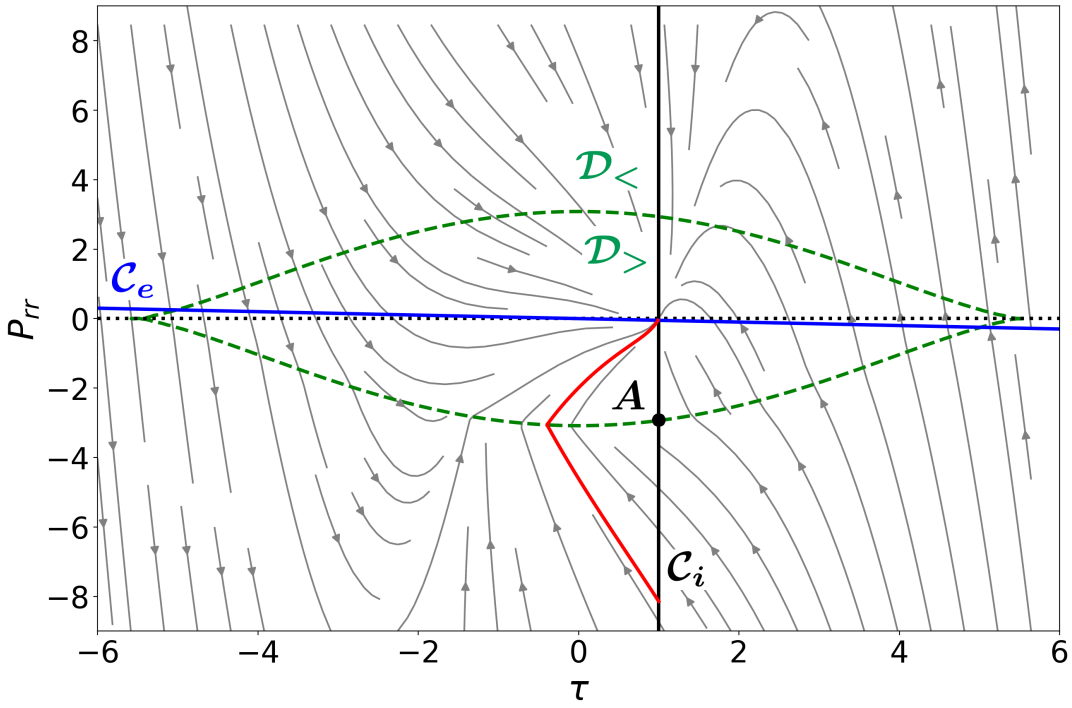

(c) Maximum real root

Figure 1: Phase portraits of the system (14) where, in $\mathcal{D}_>$, $\check{\nu}(\tau, P_{rr})$ is the (a) minimum, (b) intermediate, and (c) maximum real root of (15).

In addition, the red lines shown in Figures 1a, 1b, and 1c are trajectories of solutions of the disk problem for $\alpha = 0.001$ and $p = 0.05$. These trajectories were obtained by generating a set of points $\{(\tau^j, P_{rr}^j)\}$, $j = 1, 2, ..., N$, where $(\tau^1, P_{rr}^1) \in \mathcal{C}_i$,

$$(\tau^{j+1}, P_{rr}^{j+1}) = (\tau^j, P_{rr}^j) + \delta\xi_j \left(\frac{d\tau}{d\xi}, \frac{dP_{rr}}{d\xi}\right)\Big|_{(\tau^j, P_{rr}^j)}, \tag{18}$$

and N is such that $\sum_{j=1}^{N} \delta\xi_j = -\log\alpha$. Thus, N is the total number of steps that are necessary to go from the initial curve $\mathcal{C}_i$ to the terminal curve $\mathcal{C}_e$. We have used $\delta\xi_j = \delta\xi = 0.001$ for $j = 1, 2, ..., N-1$, and $\delta\xi_N = -\log\alpha - (N-1)\,\delta\xi$. The initial point (τ^1, P_{rr}^1) was chosen in such a way that the last point (τ^N, P_{rr}^N) is close to $\mathcal{C}_e$ within an acceptable error.

Observe from Figures 1a and 1b that the red lines end on $\mathcal{C}_e$ for τ not close to 1, which means that the outer surface of the disk undergoes a large deformation for an applied pressure that is small, which is not physically realistic. Therefore, we discard these two solutions and concentrate on the phase portrait of Figure 1c.

The solution represented by the red line in Figure 1c describes a state where the deformation is small at the outer surface and, as we approach the inner surface of the disk, the absolute value of P_{rr} monotonically increases. Although it is not shown here, we have verified that, near the outer surface of the disk where τ is close to 1, the trajectory of solution is similar to the trajectory of solution of the phase portrait obtained from the corresponding problem in classical linear theory of elasticity.

We see from Figure 1c that the trajectory changes its direction abruptly at the interface between $\mathcal{D}_>$ and $\mathcal{D}_<$. This is due to the fact that, in $\mathcal{D}_<$, the choice of $\check{\nu}(\tau, P_{rr})$ is unique, say ν^*, and, in $\mathcal{D}_>$, there are the three distinct values ν_1, ν_2, and ν_3, such that $\nu_1 < \nu_2 < \nu_3$. Along the upper green dashed line, we have $\nu^* = \nu_3$ and, along the lower one, we have $\nu^* = \nu_1$. In Figure 1c the trajectories are constructed by choosing $\check{\nu}(\tau, P_{rr}) = \nu_3$ inside $\mathcal{D}_>$, which yields a finite jump in $\check{\nu}$ along the lower green dashed line. From (14) and (9), it is not difficult to show that this jump causes a jump in both $d\tau/d\xi$ and $dP_{rr}/d\xi$, which results in a change of direction of the trajectory. Therefore, the solution r of the disk problem, represented by the red trajectory of Figure 1c, has a finite jump in its derivative r', where we recall from above that $r'(R) = \nu(R) = \check{\nu}(\tau, P_{rr})$, at an interior point of the domain $\mathcal{B}$.

The above discussion indicates that solutions having trajectories entirely inside $\mathcal{D}_>$ in Figure 1c do not have a jump in r'. In addition, for infinitesimal deformations, the response of the anisotropic St Venant-Kirchhoff material reduces to that of the classical linear theory of elasticity, in the context of which, a problem analogous to the disk problem would have a continuous r'. Therefore, we expect that there is a value of pressure, $\bar{p} > 0$, below which r' is continuous.

To determine the value of $\bar{p}$, first, observe from Figure 1c that, along the initial curve $\mathcal{C}_i$, starting points above and below the point A belong to trajectories of, respectively, smooth and non-smooth solutions. Thus, the trajectory of solution starting at point A corresponds to the pressure $\bar{p}$.

Next, at the point A, the discriminant defined by (16) vanishes, yielding the equation $D(1, P_{rr}) = 0$, from which we find $P_{rr} \approx -2.93568$. To determine $\bar{p}$ for a given α, we use (18) with $(\tau^1, P_{rr}^1) = (1, -2.93568)$ and construct the trajectory of the solution corresponding to $\bar{p}$. In Table 1, we show estimates of $\bar{p}$ calculated with different values of α and $\delta\xi$. We see that, for a given α, $\bar{p}$ seems to converge to a limit value as $\delta\xi$ decreases. In addition, for $\delta\xi = 10^{-4}$, which corresponds to our most accurate estimates of $\bar{p}$, and $\alpha < 10^{-3}$, each time we divide α by 10, $\bar{p}$ is divided by approximately 5; for instance, 5.38e-04/2.71e-03 = 5.04. This result indicates that $\bar{p} \to 0$ as $\alpha \to 0$. Therefore, if the disk is solid, that is, if $\alpha = 0$, our results indicate that the deformation field has a finite jump in its derivative r' for any value of compressive pressure $p > 0$. We do not treat the case $\alpha = 0$ directly because, in this case, $-\log\alpha = \infty$ and we cannot use (18) to obtain trajectories of solutions.

DOI: 10.5540/03.2023.010.01.0064

Table 1: Estimates of $\bar{p}$ for different values of $\delta\xi$ and α.

$\delta\xi$ \ α	10^{-1}	10^{-2}	10^{-3}	10^{-4}	10^{-5}	10^{-6}	10^{-7}	10^{-8}
10^{-1}	3.95e-01	6.40e-02	1.17e-02	2.17e-03	4.05e-04	7.58e-05	1.42e-05	2.65e-06
10^{-2}	4.22e-01	7.11e-02	1.36e-02	2.66e-03	5.23e-04	1.03e-04	2.04e-05	4.02e-06
10^{-3}	4.24e-01	7.18e-02	1.38e-02	2.71e-03	5.36e-04	1.06e-04	2.11e-05	4.18e-06
10^{-4}	4.25e-01	7.19e-02	1.38e-02	2.71e-03	5.38e-04	1.07e-04	2.11e-05	4.20e-06

4 Conclusions

We have considered the problem of a nonlinearly elastic annular disk in equilibrium without body force having uniform thickness and being fixed on its inner surface of radius R_i and compressed by a constant and uniform pressure $p > 0$ on its outer surface of radius R_e. The disk is made of a transversely isotropic St Venant-Kirchhoff material with radial symmetry axis. We have used the phase-plane method to show that the solution of this problem has a finite jump in its derivative for $p > \bar{p}$. Thus, for a given internal radius $R_i > 0$, this result yields the range of validity of the infinitesimal theory, since this theory does not admit non-smooth solutions in the interior of the body. This work is of interest in devising numerical strategies for the investigation of materials that may undergo deformed states with multiple phases. However, to use this method, we must rewrite the differential equation of the problem as a system of autonomous equations, which is not always possible.

Acknowledgments

The authors acknowledge the support of the National Council for Scientific and Technological Development (CNPq), grant n° 306832/2022-4, São Paulo Research Foundation (FAPESP), grant n° 2022/07083-8, and Coordination for the Improvement of Higher Education Personnel (CAPES) – Finance Code 001.

References

[1] R. Abeyaratne and J. K. Knowles, **Evolution of Phase Transitions**. Cambridge University Press, May 2006. ISBN: 9780521661478. DOI: 10.1017/CBO9780511547133.

[2] S. S. Antman and P. V. Negrón-Marrero, "The remarkable nature of radially symmetric equilibrium states of aeolotropic nonlinearly elastic bodies". **Journal of Elasticity** 18:2 (1987), 131–164. ISSN: 03743535. DOI: 10.1007/BF00127554

[3] I. M. Daniel and O. Ishai, **Engineering Mechanics of Composite Materials**. 2nd ed. Engineering mechanics of composite materials v. 13. Oxford University Press, 2006 ISBN: 9780195150971.

[4] S. G. Lekhnitskii, **Anisotropic plates**. 2nd ed. New York: Gordon & Breach, 1968. ISBN: 2881242006, 9782881242007.

